Compressed Sensing MRI Exploiting Complementary Dual Decomposition

Suhyung Park[1], Chul-Ho Sohn[2], and Jaeseok Park[1]

[1]*Department of Brain and Cognitive Engineering, Korea University, Seoul, Seoul, Korea,* [2]*Department of Radiology, Seoul National University Hospital, Seoul, Korea*

Introduction: Compressed sensing (CS) [1,2] exploits the sparsity of an image in a transform domain. However, it has been shown that CS suffers particularly from loss of low contrast image features with increasing reduction factor. To retain image details, in this work we introduce a novel CS algorithm exploiting feature-based complementary dual decomposition with joint estimation of local scale mixture (LSM) model and images. Images are decomposed into dual block sparse components: total variation (TV) for piecewise smooth parts and wavelets for residuals. The LSM model parameters of residuals in the wavelet domain are estimated and then employed as a regional constraint in spatially adaptive reconstruction of high frequency subbands to restore image details missing in piecewise smooth parts. Experiments demonstrate the superior performance of the proposed method in preserving low-contrast image features even at high reduction factors.

Method: Instead of directly combining wavelets with TV [2], we model an image as a union of the two complementary components: $\mathbf{f} = \mathbf{f_p} + \mathbf{f_r} + \eta$ **(1)**, where $\mathbf{f_p}$ is the piecewise smooth parts that are characterized by slowly varying baseline structures, $\mathbf{f_r}$ is the residuals retain image details complementary to the baseline structures, and η is the zero mean Gaussian noise. Exploiting the fact that TV penalty results in deformation of sharp edges and tend to smooth out oscillating boundaries [3,4], we prefer to reconstruct $\mathbf{f_p}$ using TV subject to data consistency, and then we extract complementary edge information using wavelet penalty because image details missing in $\mathbf{f_p}$ are inherently reflected in the residuals. **1) Local Scale Mixture Model:** The wavelet dependencies in both intra- and inter-scales provide a chance that similar amplitude of coefficient is to be clustered by imposing a directional wavelet-tree structure (Fig.1a) [5,6]. To reflect the spatially varying nature of wavelet dependencies, wavelet coefficients are grouped into N_p partitions over all scales, and then we propose a least-square based LSM model incorporating wavelet dependency and its non-stationary characteristics (Fig.1b):

$$\hat{\mathbf{c}}_k = \min_{\mathbf{c}_k} \left\| \mathbf{w}_{k,s-1} - \mathbf{W}_{k,[s-1\ s]}\mathbf{c}_k \right\|_2^2 + \zeta \|\mathbf{c}_k\|_2^2, \quad \textbf{(2)}$$

where $\mathbf{c}_k = \left[\mathbf{a}_k^T\ \mathbf{b}_k^T\right]$ denotes LSM model parameters representing the intra- ($\mathbf{a}_k$) and inter- ($\mathbf{b}_k$) scale dependencies belonging to the k^{th} partition. **2) Residual Reconstruction with LSM Model:** Considering the LSM model parameters as an additional constraint in residual reconstruction, we estimate a pair of high frequency subbands of residuals in the same orientation:

$$\{\mathbf{w}_{s-1}, \mathbf{w}_s\} = \min_{\mathbf{w}_{s-1},\mathbf{w}_s} \|\mathbf{w}_{s-1}\|_1 + \|\mathbf{w}_s\|_1, \quad \textbf{(3)}$$
$$\text{s.t. } \mathbf{u}_{s-1} = \mathbf{F}_u\mathbf{w}_{s-1}, \mathbf{u}_s = \mathbf{F}_u\mathbf{w}_s,\ (\mathbf{I}-\mathbf{A})\mathbf{w}_{s-1} = \mathbf{B}\mathbf{w}_s,$$

where $\mathbf{w}_{s-1}$ and $\mathbf{w}_s$ represent all wavelet coefficients in parent and child subbands of residuals, $\mathbf{u}_{s-1}$ and $\mathbf{u}_s$ denote spectral weighted data fidelity of residuals, and $\mathbf{A}$ and $\mathbf{B}$ denote the block diagonal matrices consisting of the LSM model parameters, $\mathbf{a}_k$ and $\mathbf{b}_k$over the whole partition. **3) Alternating Reconstruction of Complementary Image Components:** Both $\mathbf{f_p}$ and $\mathbf{f_r}$ are estimated by combining complementary image decomposition with the LSM model for residuals as follows:

$$\min_{\mathbf{f_p},\mathbf{f_r}} \frac{1}{2}\left\|\mathbf{F}_u(\mathbf{f_p}+\mathbf{f_r}) - \mathbf{d}_u\right\|_2^2 + \lambda_{TV}\|\mathbf{f_p}\|_{TV}$$
$$+ \sum_{o=1}^{N_o}\sum_{s=2}^{N_s}\left\{\lambda_{LSM}^{o,s}\left(\frac{1}{2}\left\|(\mathbf{I}-\mathbf{A})\Psi_{s-1} - \mathbf{B}\Psi_s)\mathbf{f_r}\right\|_2^2\right) + \lambda_1^{o,s}(\|\Psi_{s-1}\mathbf{f_r}\|_1 + \|\Psi_s\mathbf{f_r}\|_1)\right\}, \quad \textbf{(4)}$$

where $\mathbf{d}_u$ is the measured k-space data, Ψ_s is the operator that applies the wavelet transform and then extracts wavelet subband at the scale, s. Under the framework of alternating minimization algorithm, we separate the unconstrained optimization problem into two simplified subproblems, in each of which a single independent variable, either $\mathbf{f}_p$ or $\mathbf{f}_r$ exists:

$$\mathbf{f}_p^{t+1} = \min_{\mathbf{f}_p} \frac{1}{2}\left\|\mathbf{F}_u\mathbf{f}_p - \mathbf{d}_p\right\|_2^2 + \lambda_{TV}\|\mathbf{f}_p\|_{TV} \quad \textbf{(5)},$$

$$\mathbf{f}_r^{t+1} = \min_{\mathbf{f}_r} \frac{1}{2}\left\|\mathbf{F}_u\mathbf{f}_p - \mathbf{d}_p\right\|_2^2 + \sum_{o=1}^{N_o}\sum_{s=2}^{N_s}\left\{\lambda_{LSM}^{o,s}\left(\frac{1}{2}\left\|(\mathbf{I}-\mathbf{A})\Psi_{s-1} - \mathbf{B}\Psi_s)\mathbf{f_r}\right\|_2^2\right) + \lambda_1^{o,s}(\|\Psi_{s-1}\mathbf{f_r}\|_1 + \|\Psi_s\mathbf{f_r}\|_1)\right\} \quad \textbf{(6)},$$

where $\mathbf{d}_p = \mathbf{d}_u - \mathbf{F}_u\mathbf{f}_r^t$, and $\mathbf{d}_r = \mathbf{d}_u - \mathbf{F}_u\mathbf{f}_p^{t+1}$. The proposed approach, which iterates with the estimation of $\mathbf{f}_p$, the LSM model, and $\mathbf{f}_r$ in a sequential fashion, continues until the error between successive estimates becomes negligible.

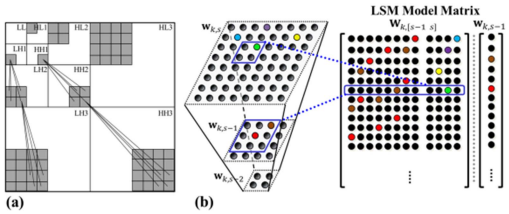

Figure. 1. *Illustration of (a) wavelet coefficients with the tree structure and (b) construction of the LSM model matrix at each partition in a pair of parent and child subbands.*

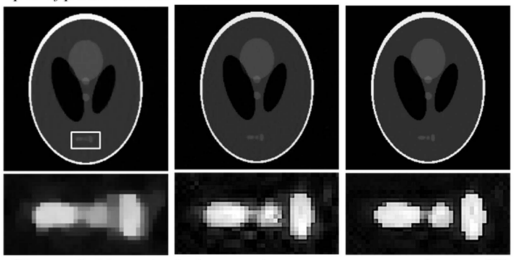

Figure. 2. *Numerical phantom images reconstructed using CS, CS-CD, and CS-CD-LSM from left to right at R=10)*

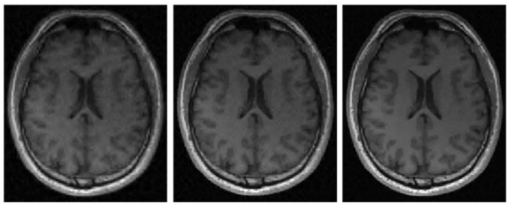

Figure. 3. *T1-weighted brain images reconstructed using CS, CS-CD, and CS-CD-LSM from left to right at R=8)*

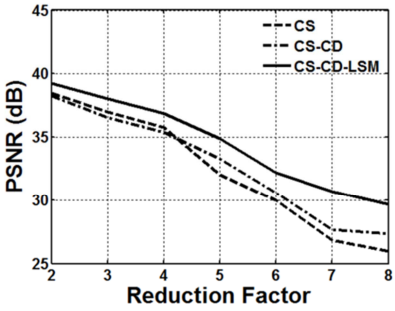

Figure. 4. *Quantitative comparison of CS, CS-CD, and CS-CD-LSM using PSNR*

Results: To validate our algorithm, numerical phantom and in vivo brain data (256x256) are simulated at R=10 and 8, respectively. To emulate under-sampling, the variable density random undersampling patterns are used. For comparison, three images are reconstructed using CS (sparse MRI [2]), CS with CD ($\lambda_{LSM}^{o,s} = 0$ in (4)) and the proposed method (CS-CD-LSM). In numerical phantom, CS and CS-CD result in severe blurring and fail to resolve three ellipses in the lower part of phantom while CS-CD-LSM delineates them more accurately with background noise suppression (Fig. 2). In in vivo brain data, with R = 8, artifacts and noise with loss of image details are severe over the entire brain image in CS, but substantially reduced in CS-CD though residual artifacts remain in the brain parenchyma. On the other hand, CS-CD-LSM restores finer details with no apparent artifacts and noise (Fig. 3). Over the entire range of R, CS-CD-LSM quantitatively achieves the highest peak signal to noise ratio (PSNR) if compared with the other two methods (Fig. 4).

Conclusion and Discussion: We show the effectiveness of the proposed CS employing complementary dual image decomposition with joint estimation of the LSM model and images. Simulation confirms that the proposed method is highly competitive against conventional methods.

References: [1] Donoho, IEEE TIT, 2006;52:1289, [2] Lustig et al., MRM, 2010;58:1182, [3] Rudin et al., Physica D, 1992;60:259, [4] Aujol et al., J. Math. Imaing. Vision, 2005;22:71 [5] Portilla et al., IEEE TIP, 2003;12:1338, [6] Crouse et al., IEEE TSP 1998;46:886.

Acknowledgements: Mid-career Researcher Program (2011-0016116) through the NRF Korea by the MEST.